MADONE WHITEPAPER

3 Executive summary

4 Introduction

5 Aerodynamic performance

17 Ride-tuned performance

25 Integration

31 Supplemental drafting study

AUTHORS Brad Addink
Paul Harder
Reggie Lund
Jay Maas
Mio Suzuki

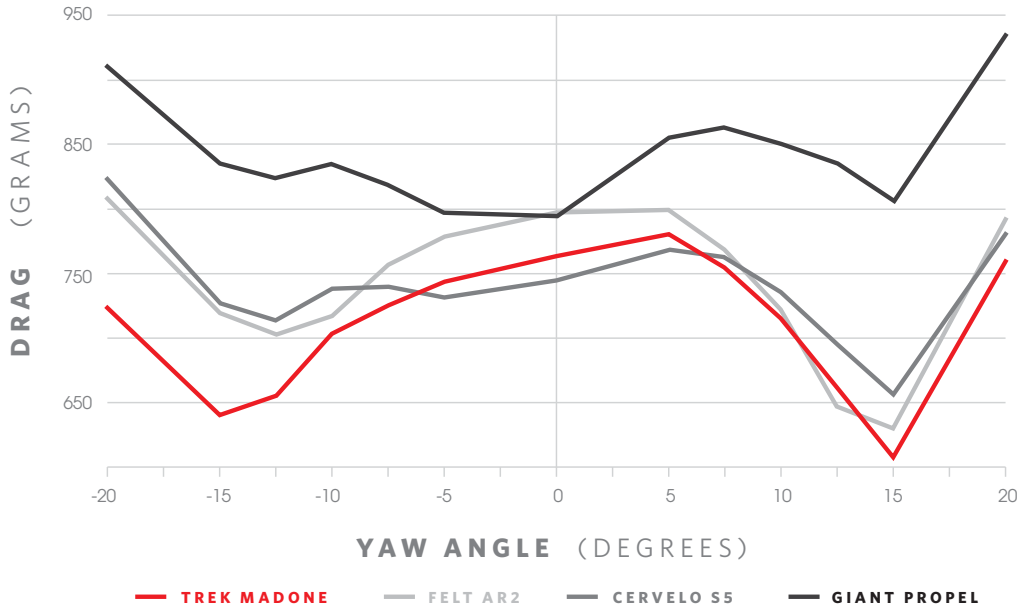

Executive summary

Trek has long been the industry leader in aerodynamics, comfort, and ride quality. We've leveraged this knowledge to create the new Madone, a bike with unparalleled aerodynamics, unmatched ride quality, and unprecedented integration.

The new Madone is not only the fastest aero bike, but it now features the proven comfort of IsoSpeed, all in a package that retains Madone's legendary ride quality. We didn't just create an aero road bike; we created the ultimate race bike.

Introduction

Trek focuses on creating technology that pushes the rider experience forward. With the goal of making you faster, Trek has continued to push the envelope with the often copied but never duplicated Kammtail Virtual Foil. Through the use of FEA and CFD, the new Madone has set a new benchmark for bicycle aerodynamics.

Trek recognized going into the project that having the most aerodynamic bike would not be enough. Aero bikes are known for their harsh rides and poor handling, and we knew that a bike will not make you faster if you don't want to ride it. We had to do something different—so the foundation of the project centered on the proven comfort of the IsoSpeed system. Combining IsoSpeed technology with hundreds of Finite Element Analysis (FEA) simulations Trek has created at bike that powers through the sprints and handles smoothly, carving through the most demanding corners.

Aerodynamic performance

CFD

Computational Fluid Dynamics (CFD) has been a prevalent tool within the bike industry for years. In recent years, Trek engineering has accelerated the pace of product development by reinventing the way CFD is used. Through the use of cloud-based cluster computing, and the most advanced commercial CFD software (STAR-CCM+,) and rigorous wind tunnel correlation, Trek has brought about a complete paradigm shift in the way CFD is used to optimize bicycle aerodynamics.

In this section, we describe the general methodology for frame and component development. Trek uses CD-adapco's STAR-CCM+ (v7.02 – v9.06) for CFD analysis. Like all commercial CFD tools, STAR-CCM+ numerically solves sets of mathematical equations that describe motion of fluid (air).

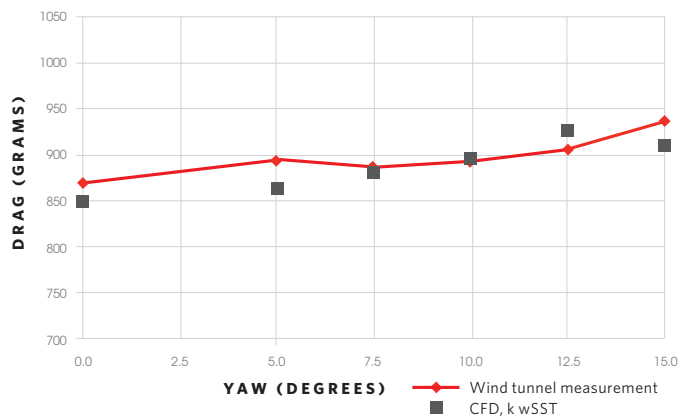

Figure 1. Wind Tunnel Result (SD LSWT, October 2011, Run 7 2013 Madone) vs. CFD model

CFD using wind tunnel data

We rigorously calibrated CFD prior to the project frame analysis so that the computational results accurately portray the outputs of experiments. Choosing the correct turbulence model, fine tuning the model parameters, and conducting extensive mesh convergence studies are essential to accurately capture the flow dynamics around a bicycle. One of the calibration results comparing the wind tunnel drag vs. CFD drag on previous Madone is shown in figure 1. In this particular example, CFD accuracy is within 3% of the wind tunnel result.

Design iteration process

With the CFD model properly set for bike analysis, we began a series of frame analyses. A typical analysis consists of a simplified bike with or without a mannequin model in a simulated wind tunnel. For steady-state simulations, wheel rotation was modeled by imposing moving reference frame in the rotation domain, and specifying the local rotational velocity at the edge of the tire. The inlet boundary is specified to have an uniform air velocity at 30mph, and all the walls in the model are sufficiently resolved to capture boundary layers and viscous sub-layer effects. A typical bike-in-a-tunnel simulation would contain roughly 12 million volume cells. In order to reduce the simulation turnaround time, the simulations were solved on a remote cloud HPC cluster (R Systems NA, Inc., www.rsystemsinc.net) using 128–256 cores.

The main benchmarking quantity was drag force on the bike computed in the direction of its axis. Additionally, we monitored the following quantities to identify drag reduction opportunities:

- Surface flow separation tendency
- Low-energy eddies near the bike surface
- Amount of wake turbulence
- Local and accumulated force on wheel, fork, frame, and components

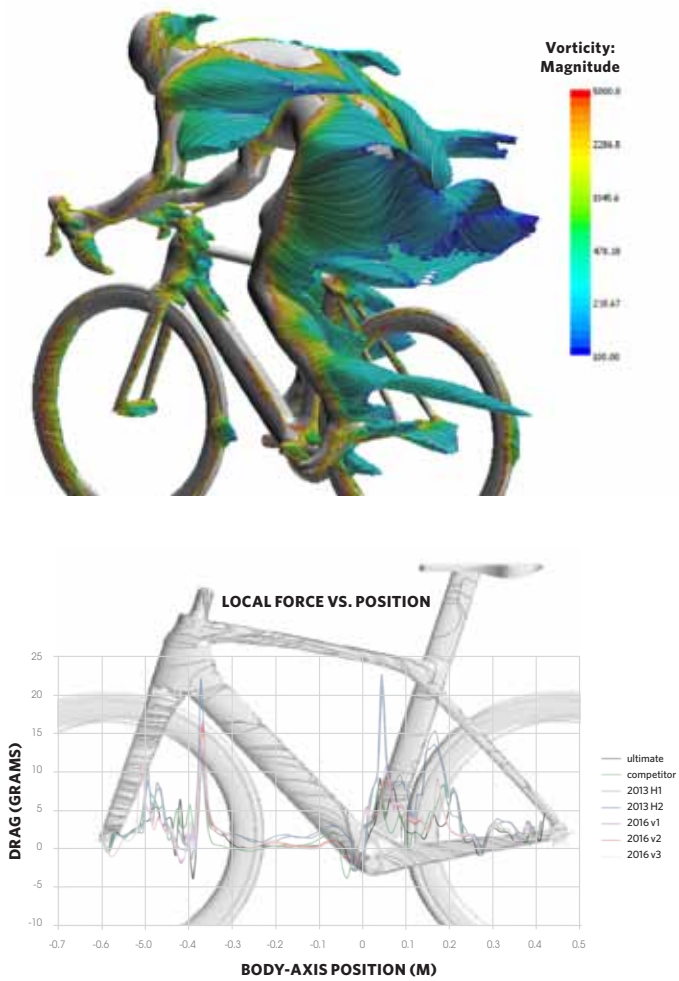

Figure 2. An example of (top) flow separation visualization and (bottom) local force vs. frame axial position plot

Analysis of the frame tubes

From the baseline frame, each iteration targeted areas that have the most impact on the overall bike drag.

We employed adjoint method to identify the areas where frame geometry change would heavily influence the axial momentum of the air, and resulting pressure force distribution on the frame. This sensitivity analysis is useful in determining the target areas early in the analysis process.

Modifications on BB lug, down tube, head tube, seatmast, seatstays, and seat tube are reflected in the drag reduction from the baseline design to one of the prototypes. The table below summarizes the reduction in each area. A tunnel test from October 2012 validates this design change effort.

Figure 3. Adjoint model, axial-momentum sensitivity volume sample overlaid on frame pressure map

DRAG REDUCTION (GRAMS), YAW = 7.5 DEG

CFD	Part	Proto A	Proto X	Drag Reduction
	BB Lug	44	29	14
	Down Tube	83	55	28
	Head Tube	48	43	6
	Seat Mast	90	33	57
	Seat Stays	55	49	6
	Seat Tube Lug	114	61	53
	Totals:	*434*	*270*	*164*
Wind Tunnel (October 2012)	**Part**	**Proto A**	**Proto X**	**Drag Reduction**
	Complete bike	*899*	*741*	*158*

Table 1. Drag reduction on various frame parts from Proto A (baseline) to Proro X (grams)

Figure 4. Proto A (left) vs. Proto X (right) — wall shear vector

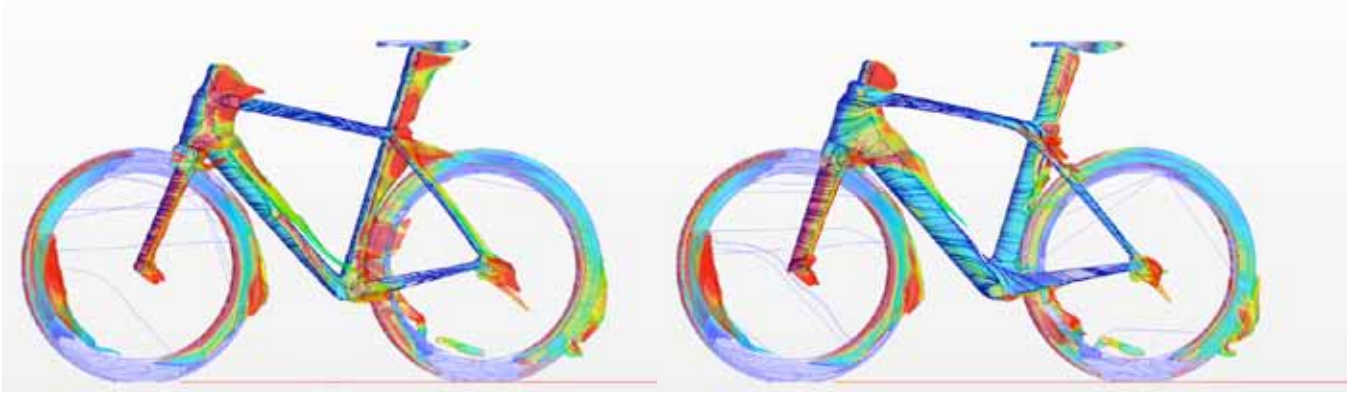

Figure 5. Relative pressure iso contour (color = turbulent kinetic energy). Benchmarking bike (left) vs. Proto v2 (right)

The majority of improvements on the frame tubes come from understanding the flow separation tendency on the selected tube surfaces. By analyzing the momentum/kinetic energies that the air carries when flowing over these surfaces, we can predict the relative pressure change. Carefully modifying the surface contours and selectively using kammtail where appropriate helps to sustain the energetic air flow by avoiding drastic pressure change, thus achieving better aerodynamics.

After rounds of wind tunnel verifications, we focused further prototype improvements on the components and minor changes on the frame. The redesigned front brake and fork ensure the continuous air flow toward the down tube. Bar/stem redesign hides the cables from the front end, erasing the cable drag that can account as much as 37 grams over 0-15 degrees (wind tunnel measurement: November 2013). The smooth profile on the new bar/stem also allows for efficient air flow and minimizes unwanted eddies. The wind tunnel measurement (October 2012) indicates that the new bar saves ~34 grams of drag (0-20 degrees yaw average) when compared to the current Bontrager XXX Aero bar as shown in figure 6.

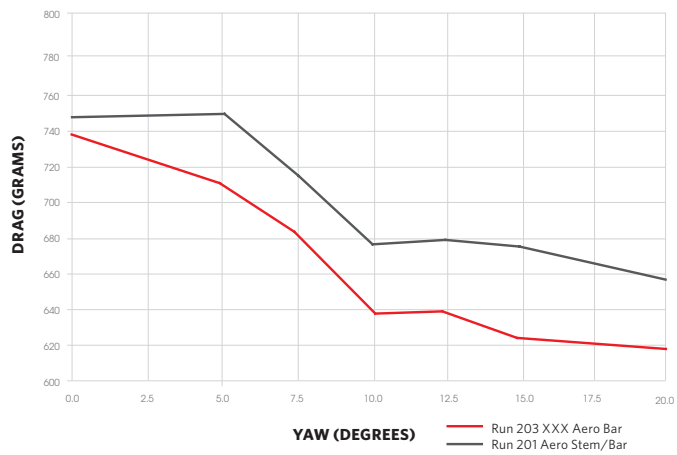

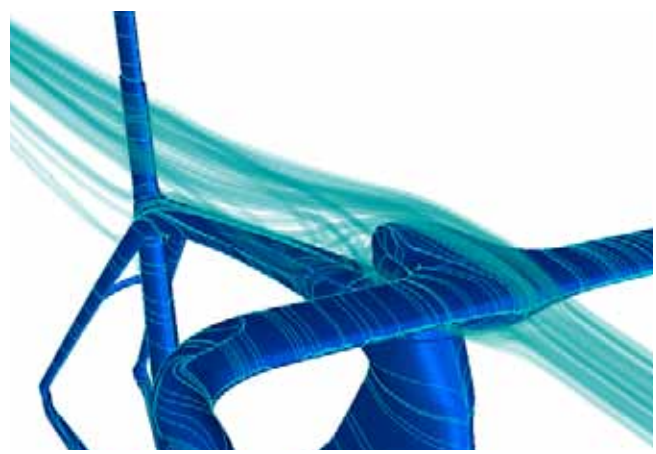

Figure 6. Wind tunnel measurement comparing Bontrager XXX Aero vs the new Madone's stem/bar (top), and CFD flow visualization on the new stem/bar (bottom)

THE NEW BAR SAVES ~34 GRAMS OF DRAG WHEN COMPARED TO THE CURRENT BONTRAGER XXX AERO BAR

WE PERFORMED 140 ITERATIONS IN THIS STUDY. THE FINAL RESULT SHOWED A 5.5% REDUCTION IN THE OVERALL DRAG

Water bottle placement optimization

We set out to make Madone the fastest bike under real-world conditions—which meant analyzing the impact of water bottles on aerodynamics. The addition of down tube and seat tube water bottles impacts drag by creating additional pressure and disrupting the air flow on these tube surfaces (figure 8). To minimize these unfavorable drag impacts, the locations of the bottles were derived using algorithm-based optimization software.

Red Cedar Technology's HEEDS is an optimization software that integrates with CAE tools to drive adaptive optimization search. We used HEEDS to explore the optimal water bottle locations on down tube and seat tube to minimize overall frame drag.

In the starting CAD, water bottles were mounted on down tube and seat tube at arbitrary points on a prototype frame. Each bottle's original location was marked with respect to the center of the bottom bracket. HEEDS would then iterate over new designs (new bottle positions), progressively adjusting the iteration input values according to the prior drag responses. We performed 140 iterations in this study. The final result showed a 5.5% reduction in the overall drag.

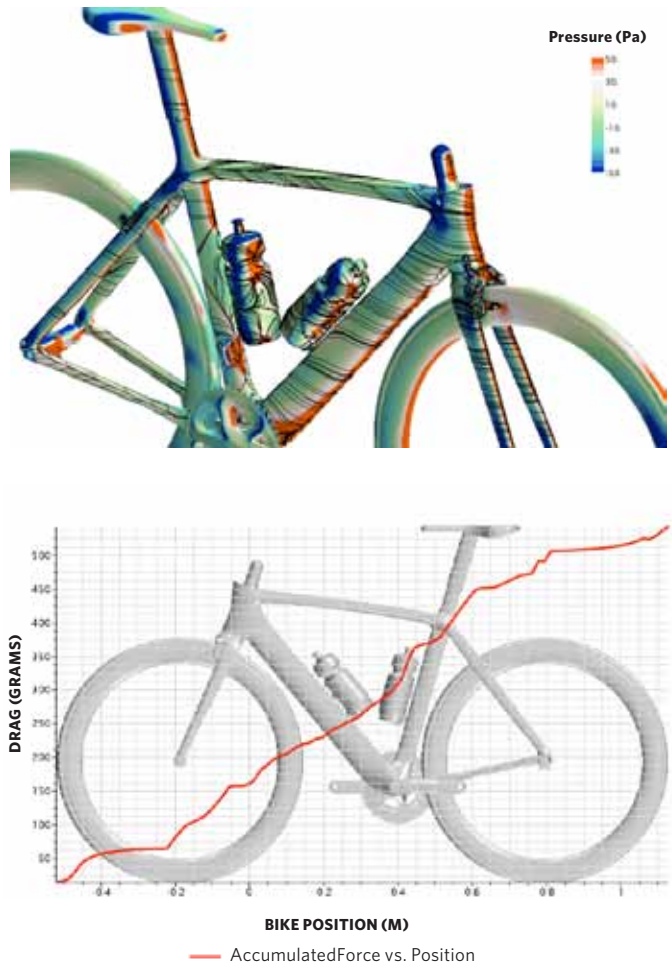

Figure 7. Impact of the water bottles on the surface pressure and surface flow (top), and accumulated drag force vs. bike position (bottom)

One of the great advantages of incorporating an automated optimization method comes from its ability to offer ensemble-based analysis. Trends for achieving the objective become apparent once sufficient data are produced via design exploration.

For this study, the aggregate result showed the preference to place the seat tube bottle as low as it can toward the BB, while keeping its influence minimal on the down tube. The seat tube is an important area for determining the overall bike drag and affects the bike's yawing ability, so keeping this tube as exposed as possible would minimize the drag penalty.

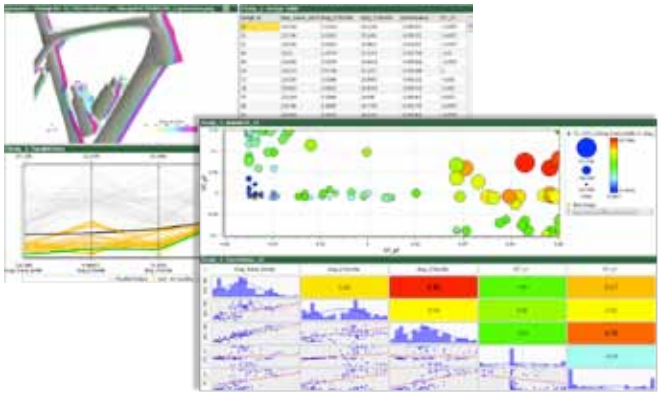

Figure 8. HEEDS outputs for water bottle placement optimization

Figure 9. Wind tunnel bike set up. San Diego Low Speed Wind Tunnel, 2015.

Low-speed wind tunnel testing

Trek's wind tunnel testing protocol is the foundation for our bicycle airfoil development and validation. Trek engineers adhere to strict standards developed over 15 years of using low-speed wind tunnel testing to validate CFD results, test different airfoil shapes, and compare our bike to the best competition in normalized configurations.

For these tests, the normalized configuration consisted of setting up all bikes in the same position as Madone's lowest position. We set shifter location and saddle height/angle/rotation as close to identical as possible. We kept most other aspects of the bikes consistent (drivetrain parts, tires, wheels, etc.) but retained each company's bar and stem setup. We used Shimano Ultegra brakes for all non-integrated brake setups.

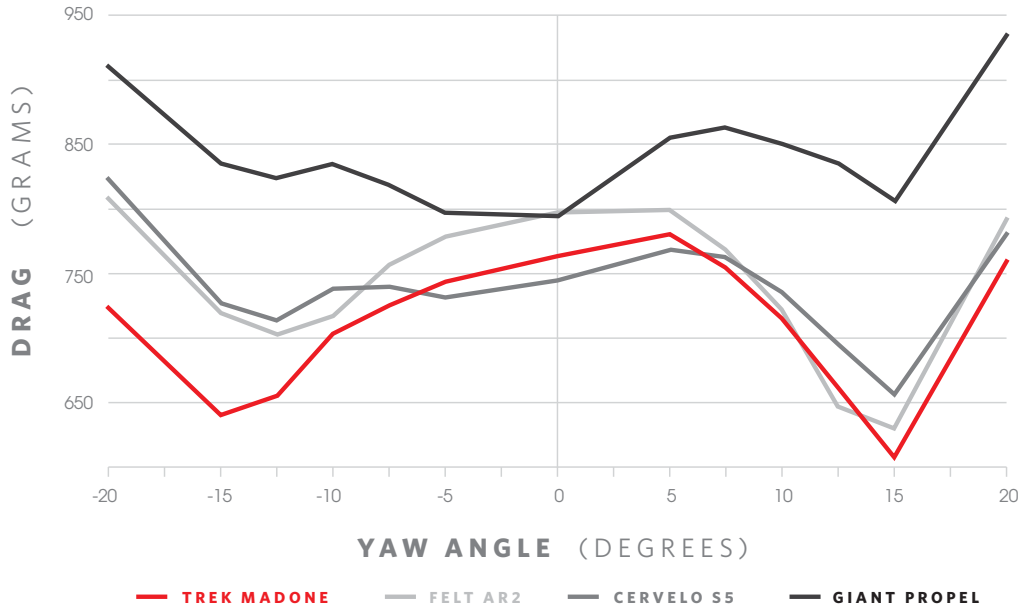

Figure 10. Wind tunnel data

The head-to-head wind tunnel comparison (figure 10) used water bottles on both the down tube and seat tube. This configuration represents a very common configuration used on road bikes. As laid out in figure 10, Madone is the overall fastest bike across all yaw angles. Note: we did not test the Specialized Venge during this trip based on data collected from previous test that showed it was not a leader in aerodynamics.

WE DID NOT TEST THE SPECIALIZED VENGE DURING THIS TRIP BASED ON DATA COLLECTED FROM PREVIOUS TEST THAT SHOWED IT WAS NOT A LEADER IN AERODYNAMICS.

Yaw	Madone	Standard Road Bike	S5	Propel	Felt AR
-20	723	1348	823	911	809
-17.5	682	1265	774	873	764
-15	641	1183	725	835	720
-12.5	655	1135	714	824	703
-10	704	1113	738	835	717
-7.5	726	1087	740	819	757
-5	744	1060	732	797	779
-2.5	754	1048	738	796	788
0	764	1037	744	795	797
2.5	772	1078	756	825	798
5	781	1119	768	855	799
7.5	755	1143	762	863	769
10	715	1170	736	850	722
12.5	662	1166	695	836	647
15	608	1196	656	807	629
17.5	684	1264	718	871	711
20	759	1332	780	934	792
Average	713	1161	741	843	747
Δ from Madone	0	448	28	129	34

Table 2. Grams of wind tunnel drag. Yaw data highlighted in red is interpolated from data trend lines

WATTS SAVINGS VS. STANDARD ROAD BIKE

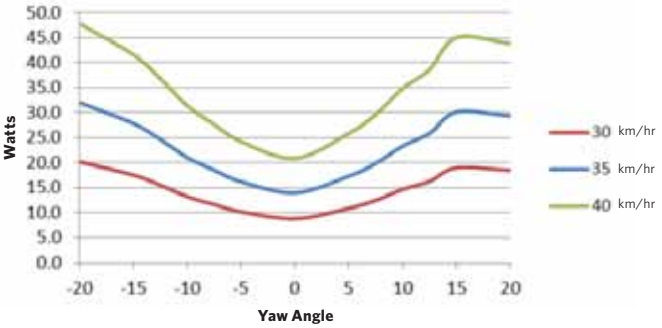

Figure 11. Comparison chart of wind tunnel results, calculated for a typical 56cm rider

TIME SAVINGS PER HOUR VS. STANDARD ROAD BIKE

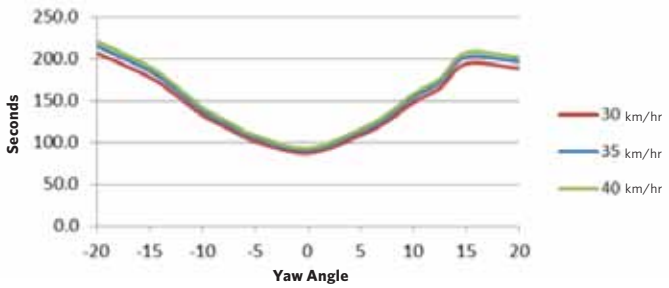

Figure 12. Comparison chart of wind tunnel results, calculated for a typical 56cm rider

To give a sense of what this means to the rider, figure 11 plots the watts savings going from a road bike to the new Madone across the entire yaw range based on a 56cm size rider (CdA of 0.3). This can be translated into seconds saved per hour of riding, shown in figure 12.

Velodrome testing

In January of 2014 we took the prototype Madone to the Mallorca Velodrome to test with the Trek Factory Racing team. Using our Alphamantis track aerodynamics testing system, we measured the difference between theMadone prototype and a standard road bike, riding solo and while drafting.

First, we tested both bikes with the rider solo and found that the Madone prototype had a 19W advantage over the standard road bike, as shown in Figure 13. This real-world result agreed very well with the wind tunnel.

Next, we tested both bikes with the rider drafting. Clearly, the effect of drafting is massive, cutting the rider's power in half. But despite the reduction in total power, a significant portion of the Madone prototype advantage remained. This test was our initial indicator that an aero bike retains an appreciable advantage, even when drafting.

As an additional point of interest, notice how the rider's power solo on a TT bike was roughly halfway between solo on a road bike and drafting on a road bike.

Of course, the indoor velodrome is an idealized environment compared to the outdoor race conditions for which Madone was designed.

So, as a next step in our drafting research, we have begun testing the Madone in various drafting formations out in the real world. The details of these tests can be found in the supplemental drafting study.

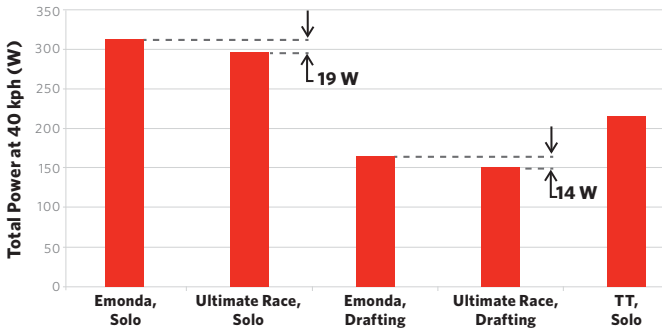

Figure 13. Bikes were normalized to the same position and ridden by the same rider. Actual test speeds ranged from 40-42 km/h, and the data was then normalized to 40 km/h.

Ride-tuned performance

Madone IsoSpeed

Aerodynamic tubes shapes typically have high aspect ratios, where the depth of the tube is two to three times greater than the width. This provides for a very aerodynamic profile, but the large section properties resist bending, like an I-beam, creating a harsh and unforgiving ride. The ultimate race bike couldn't sacrifice one for the other, so we needed to find a better way.

The first idea was to add the IsoSpeed system to an aero tube profile, but because of the high aspect ratio of the tube there would still be minimal compliance in the system, even with the added degree of freedom IsoSpeed provides.

The solution was to separate the aerodynamics and the comfort with our tube-in-tube construction. This new way of constructing a frame allowed us to design an outer tube structure optimized for aerodynamics with KVF tube shapes, and an inner tube optimized for comfort. Figure 14 shows an FEA section cut of the new Madone. The image shows how the internal tube of the IsoSpeed system deflects and maintains the excellent vertical compliance Madone is known for. The result: an incredible 57.5% improvement in vertical compliance over the nearest competitor.

Figure 14. Vertical compliance finite element analysis of Madone prototype

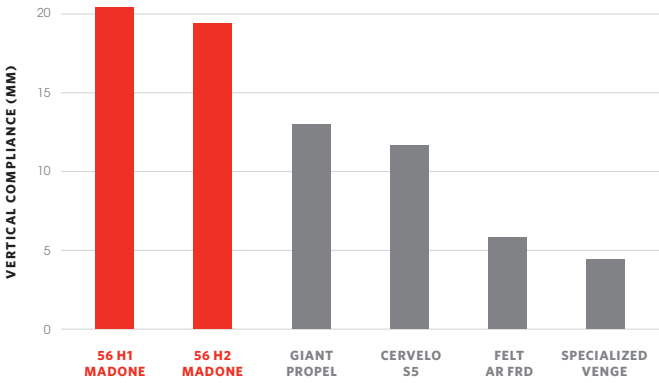

Figure 15. Vertical compliance of aero road bikes

Rides like a Madone

For the last several years, the Trek engineering team has undertaken a significant effort to understand the road bicycle loading environment during real-world riding events. This understanding is crucial to ensure that a frame with deep aggressive tube shapes, such as the new Madone, maintains the ride quality Madone is known for. The industry performs many standard tests in the laboratory to assess stiffness of frames and makes assumptions about ride quality based upon those stiffness numbers.

At Trek, however, we believe that stiffness alone cannot be used to determine a bicycle's ride quality. For example, we have created and tested frames with identical Tour BB stiffness values that exhibit different riding characteristics. This difference is not only noted by our test riders but is also shown by a cornering Finite Element Model. As shown in figure 16, four test frames displace differently during cornering even though they have the same Tour BB stiffness value. Through extensive ride testing and correlation to lab tests we have determined the need for an additional test that accurately predicts ride quality during high speed cornering

Fundamentally understanding the loading environment, how the bicycle behaves during these loading events, how the frame centerline, tube shapes, and laminate design effect this behavior, and finally correlating these aspects of frame design to rider preferences are all essential to creating the ultimate race bike.

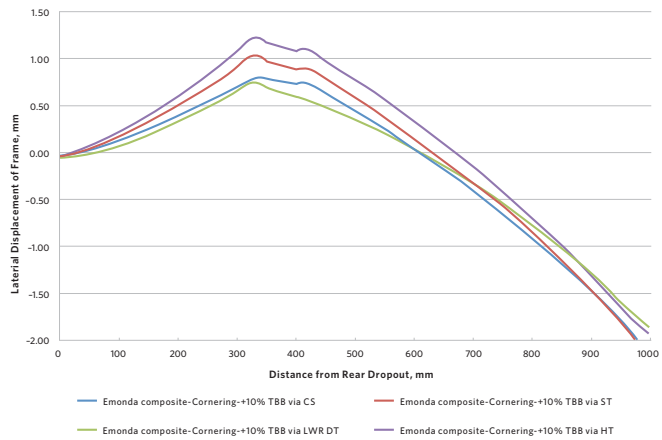

Figure 16. Lateral displacement of Emonda test ride frames predicted by cornering finite element model.

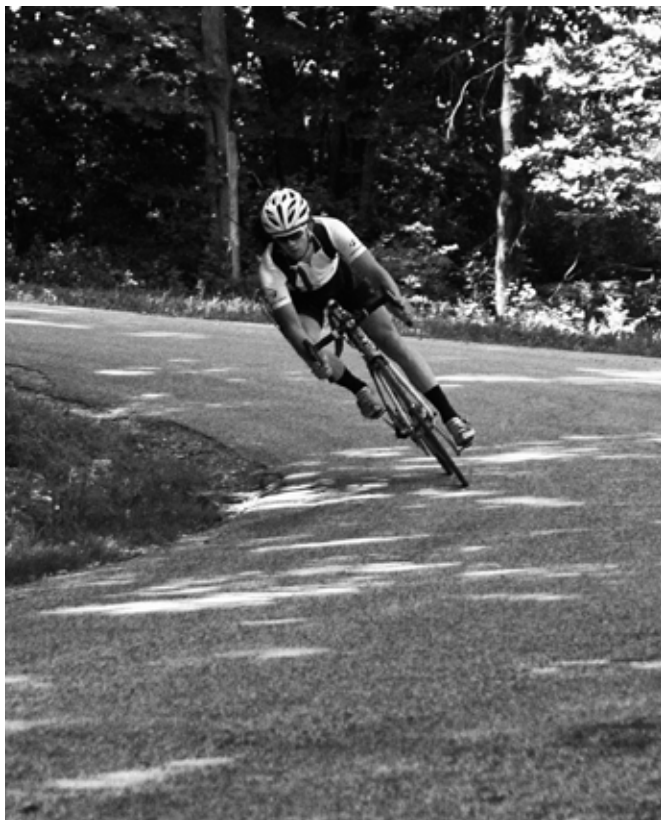

Figure 16. Test bicycle during standing climbing and cornering loading events.

Developing the cornering FEM

Trek has used a test platform consisting of a straight gage aluminum frame instrumented with strain gages, accelerometers, a power meter, and speed and cadence sensor. The test data, used in conjunction with Abaqus/CAE finite element models (FEMs) and the True-Load post processing tool, allow us to determine the loading environment throughout the event of interest and to correlate measured strains to strains predicted by the new cornering FEM.

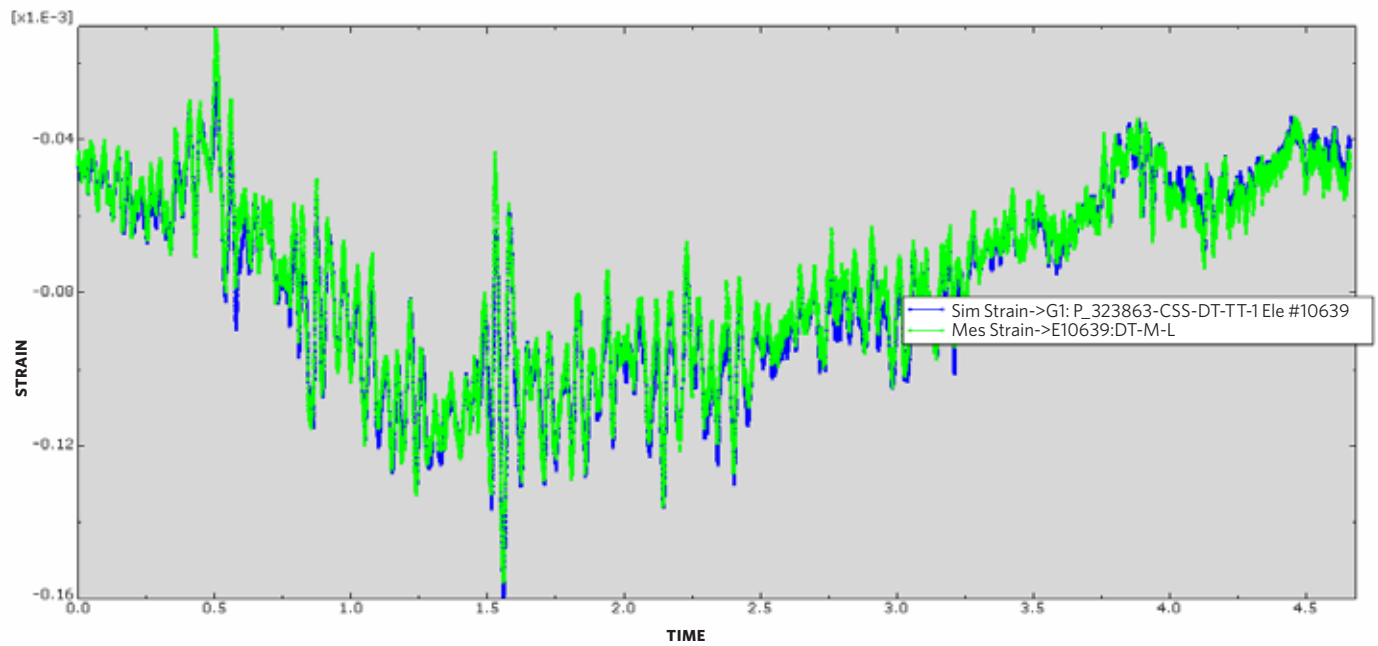

Figure 17. Middle non-drive side down tube strain during cornering load case. Simulated strain in blue (Finite Element Analysis) as compared to measure strain in green (in the field). Note only 3% error between measured and simulated strain.

Figure 17 shows strains that occur in the middle non-drive side side of the down tube during a high speed cornering event. The green curve shows the measured strains while the blue curve shows the strains as determined by the finite element model. As the image shows, the FEM is accurately predicting strains, which means the FEM can reliably be used as a tool to predict bicycle behavior in the real world.

We used the new high-speed cornering model in conjunction with the traditional stiffness models to assess design iterations and ultimately to help determine the laminate used for the new Madone. Figure 19 shows displacement curves for Émonda, the 2016 Madone early prototype, and an extra-stiff prototype 2013 Madone. Out-of-plane displacements are shown for the chainstays and down tube as extracted from the FEM results.

We had completed extensive ride testing on Émonda to achieve its fantastic ride quality, and we now conducted additional ride testing to correlate those ride characteristics to the new cornering model. As can be seen in the chart on the right, the down tube displacement for the new Madone is very similar to Émonda. The extra-stiff prototype 2013 Madone is shown here as a comparison because of its known poor ride characteristics.

CORNERING – Uz DISPLACEMENT OF CHAINSTAYS

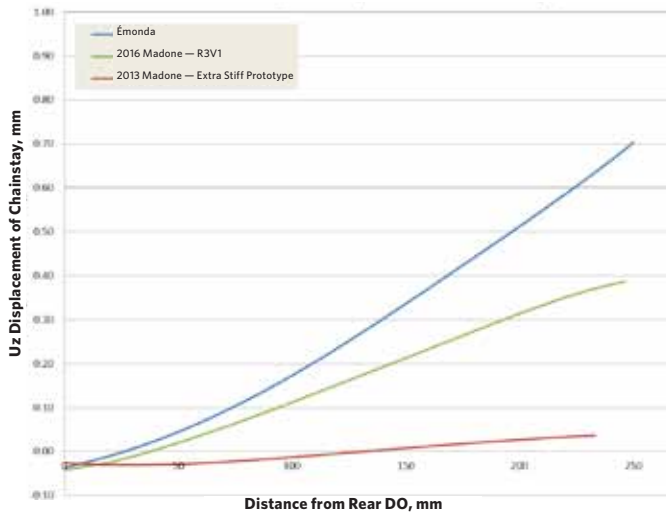

CORNERING – Uz DISPLACEMENT OF DOWN TUBE

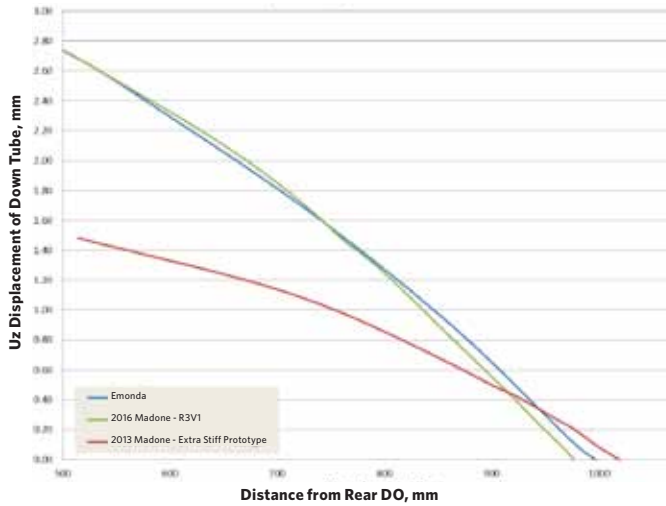

Figure 19. Displacement curves from high-speed descending FEM. CS displacement (top) and DT displacement (bottom).

THE DOWN TUBE DISPLACEMENT FOR THE NEW MADONE IS VERY SIMILAR TO ÉMONDA

Correlating the ride test

Accurate FEMs, developed and validated using measured strain data, were an important first step in the new Madone development process. But without a correlation to reality, the laboratory and FEM data is just that: data. Crucial to maintaining the legendary Madone ride quality was the correlation of stiffness numbers and FEA data to rider feedback and preferences.

We completed exhaustive ride testing during the research and design phase to understand laminate effects on ride quality (high-speed cornering, sprinting, climbing, comfort). Those same laminate changes were made in the FEMs, and the effect on stiffness and bicycle behavior was determined and correlated back to the rider feedback. This information was used to assess the effect on ride quality of tube shape and laminate changes during the new Madone development.

During the prototype phase we analyzed over 45 design iterations for many load cases each, resulting in many hundreds of finite element analysis runs. For each of these iterations we assessed stiffness and ride quality and balanced them against the aerodynamic gains or losses. As mentioned above, aerodynamics were of utmost importance for the new Madone, but we did not sacrifice ride quality.

Trek Factory Racing validation

We took full advantage of the Trek Factory Racing team throughout the development process to ensure the continuation of Madone's racing heritage. In January of 2014 the TFR team rode the Madone prototype in Mallorca, Spain. We provided the team with three unique laminates and tested all aspects of the bike's performance while climbing and cornering down the mountains. The feedback from the team led to the creation of an additional size prototype frame and new laminates for followup testing in March near Livorno, Italy (Castagneto Carducci). After the Livorno testing, the most common feedback we got from the team was: How quickly can we have the production bike to race?

Team feedback on the Madone prototype confirmed that we were on the right path for the production bike. As we finalized the details, we knew we still needed to fine tune the laminate. The bike handled great, but we needed to make sure every detail of the handling was confirmed. In December 2014 we took the full production bike to the team with three laminates to choose from. The final ride test took place in January 2015.

Integration

Designing the most aerodynamic race bike from the ground up required unprecedented integration. We left no stone unturned, no cable in the wind. The result is the most integrated road bike ever with invisible cable routing.

Brakes/forks/vector wings

The front end of the bike is the first section to interact with the wind, which makes it critical in aerodynamic behavior and sets the stage for the rest of the bike. The fork uses our proven aerodynamic KVF legs, cheating the wind at all yaw angles while maintaining stiffness for unmatched cornering ability. The fork crown is pocketed out for smooth integration with the front brake, and the fork uses a proprietary steer tube shape to allow internal routing of the housing through the top headset bearing.

The brakes have been designed to seamlessly match the fork and seatstay surfaces, integrating with the recessed areas and allowing air to flow smoothly over the entire surface. The housing of the front center-pull brake is routed down the front of the steer tube through the head tube and to the brake, all fully internal. With the same center-pull design, the rear brake housing passes through the top tube with a stop at the seat tube, allowing only a small length of brake cable to be exposed to the wind.

The brakes have been designed with functionality in mind. The quick-release levers front and rear allow for easy wheel removal. The slotted front brake housing stop allows for travel breakdown without disconnecting the wedge, making setup at the destination as easy as placing the wedge back in the brake.

The brake arms use independent spring tension adjustment screws to center the brake pads and adjust lever pull force to the desired feel. Additionally, two spacing screws allow for precise pad adjustments as brake pads wear. The spacing screws' range allows swapping between rims with up to 6mm difference in width without adjusting the center wedge.

Madone's Vector Wings protect the front brake from the elements to ensure consistent braking function. To accommodate the function of the center pull brakes, the Vector Wings articulate during turning in order to allow free rotation. As part of the seamless integration of the Vector Wings into the head tube shape, each Vector Wing is painted to match the bike.

Bar/stem

Full internal cable routing required us to rethink the stem/handlebar interface. The first step was combining the bar and stem into a single piece, using the KVF tube shaping to improve the aerodynamics over a separate system. Keeping the housing fully internal through the head tube required the design of an integrated top cap cover and spacers. The headset spacers use a two-piece clamshell design for easy adjustability, allowing addition or removal without rerouting any housing or cables.

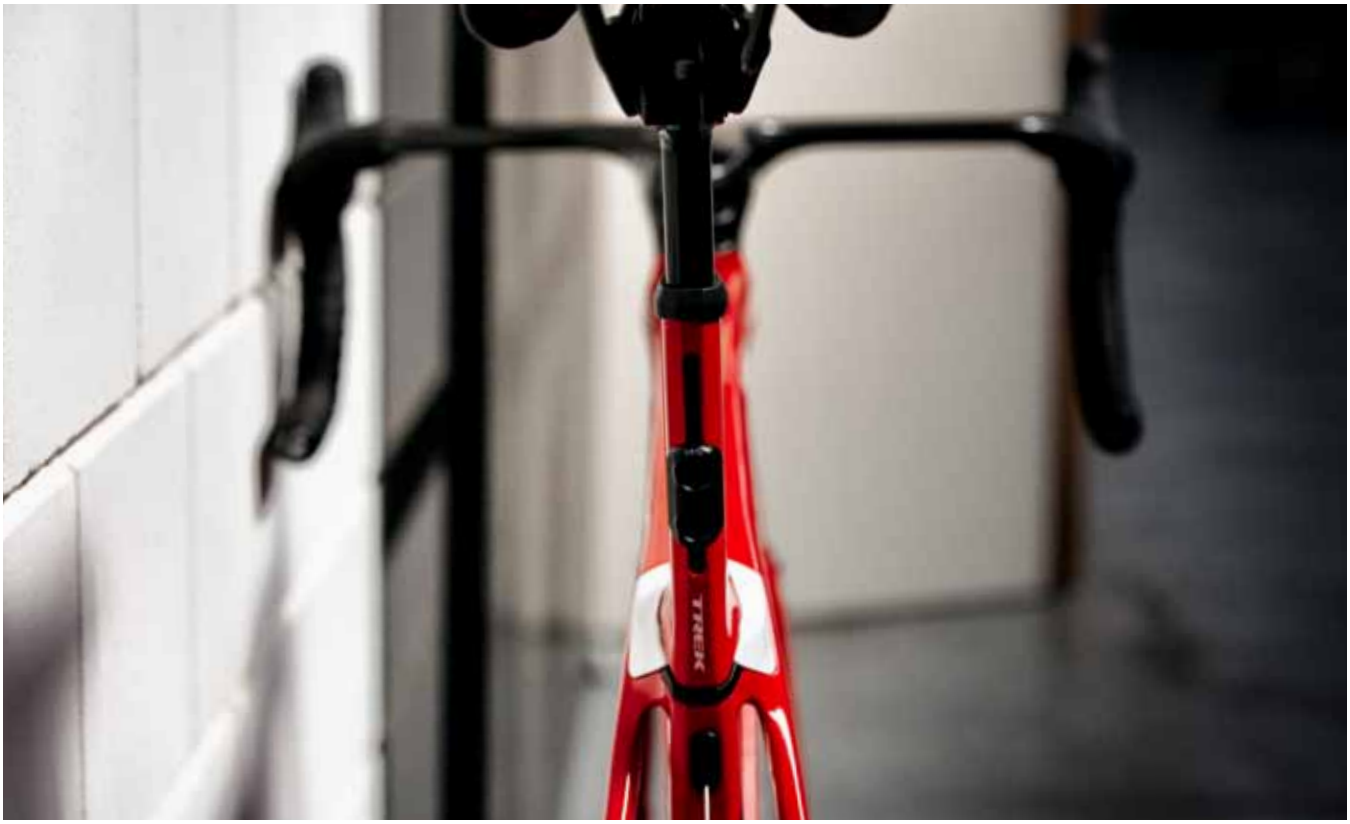

Seatpost

Using the IsoSpeed system freed up the seatpost to use Trek's proven KVF technology, matching the wind-cheating seat tube profile and maintaining class-leading compliance.

The seatpost head uses an independent pinch bolt and rail clamp system to allow for infinite tilt and setback adjustment. Snap-on rear reflector and light brackets integrate safety seamlessly into the design.

Control Center

To maintain fully internal housing while preserving the ability for easy adjustments, Trek created the Madone Control Center, located on the down tube and painted to integrate seamlessly with the bike. On mechanical setups, the Control Center houses the front derailleur trim dial.

For electronic setups, the Control Center locates the Di2 battery and junction box in one location, providing access to the trim button through the window in the top of the Control Center. Charging is made easy with a simple one-tab release to expose the charging port.

Single pace line formation

Supplemental drafting study

Test procedure & results

Following the drafting test in the indoor velodrome, we set out to quantify the effects of drafting in a variety of real-world road racing conditions, including the effects of wind. For this test, we found a flat, unobstructed, low-traffic road near Janesville, Wisconsin. At this location, we could test one-minute continuous increments in an out-and-back "L" course, achieving four unique directions relative to the wind.

We conducted testing on one day where the ambient wind averaged 7 km/h & yaw angles averaged 6 degrees, and on another day where the wind averaged 15 km/h & yaw angles averaged 15 degrees. On each day, we tested bike speeds ranging from 30–40 km/h and various drafting formations ranging from 2 to 9 riders. Again, the goal was to capture a wide variety of real-world road racing conditions.

The figure below shows some of the drafting formations we studied, ranging from a 2-man break to a 9-man simulated peloton. As a separate study, we measured the effect of drafting distance in the 2-man formation as described on page 35.

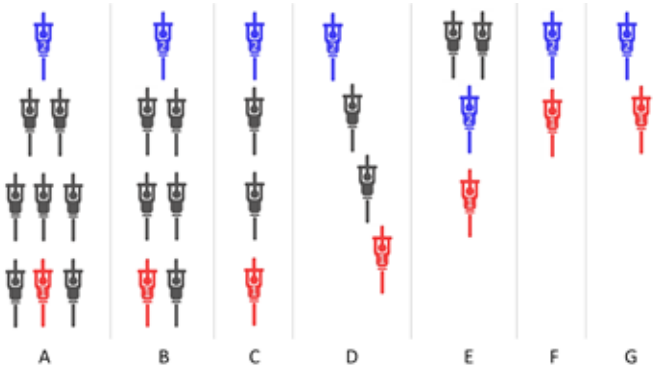

Diagram of example drafting formations tested

Aerosticks mounted to the leading and drafting riders' Madones

We collected standard speed, power, and GPS data—but the key test data came from two Alphamantis Aerosticks, one mounted to formation's most exposed leading bike (blue bike above) and one to the most protected drafting bike (red bike above).

Each of these Aerosticks gives the total airspeed and yaw angle of the air coming into the front of the bike. These simultaneous two-bike measurements revealed drafting's effect on yaw and airspeed. This method requires excellent calibration and agreement between both Aerosticks, so these sensors were validated in a separate study described on page 36.

It is important to note that in this test, we are measuring the airspeed and yaw at the single point in space at the end of the Aerostick sensor tip (at the front edge of the front wheel, at roughly head-tube height). This is the typical location for aero probe testing because it is down and away from the rider's own pressure front. While this is great for measuring the uniform field of "clean air" impinging upon the lead rider, it is only one point of reference in the chaotic wake impinging upon the drafting rider.

Typically, this forward/centered point is in the very best part of the draft, leading to quite low airspeed measurements. However, we believe that these tests still yielded interesting results and trends worth publishing.

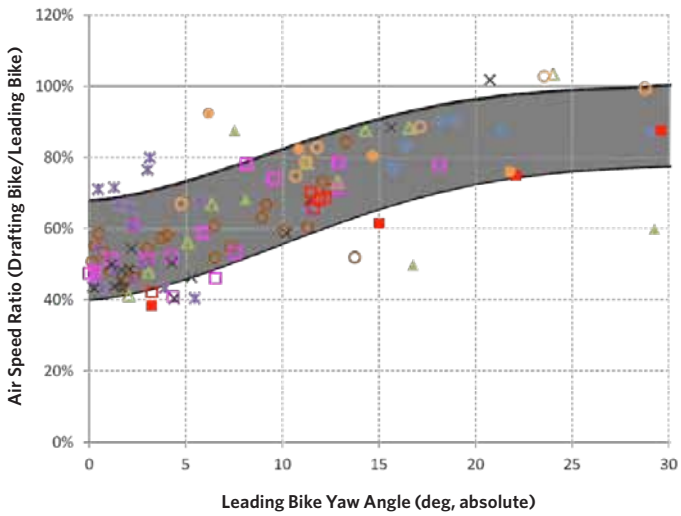

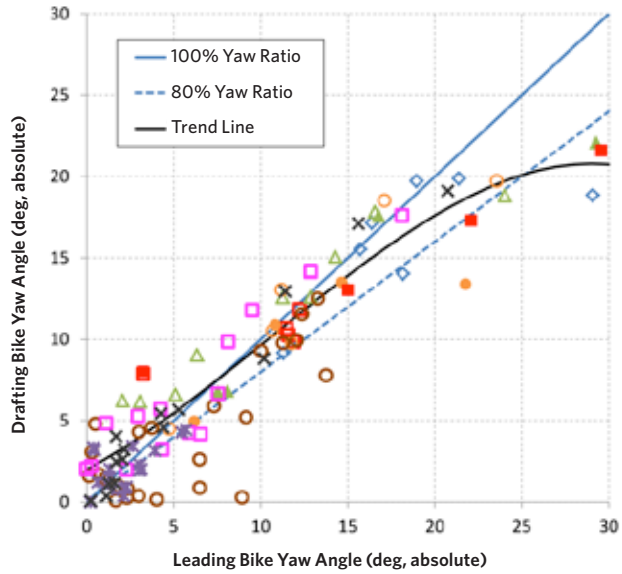

Trend of the airspeed ratio vs. yaw angle, with each style of data point representing a different drafting formation. The grey region indicates the general trend. This trend can also be seen in the raw data, as shown on page 40. For explanation of airspeed ratios greater than one, see page 39

As we see above, the drafting bike's airspeed is around half of the leading bike's airspeed at low yaw angles. However, at more typical yaw angles in the 5–15 degree range, the drafting bike sees about 60–80% of the leading bike's airspeed. Beyond 20 degrees yaw, the drafting effect becomes generally more minimal and sporadic.

We also see above that drafting has a much smaller effect on yaw angle, but a slight trend can be distinguished. In all but one of the drafting formations, the yaw angle was slightly increased at low yaw. This effect is due to the increased fluctuation in the draft as shown on page 38. In the 5–20 degree yaw range, drafting has little effect on yaw angle. Beyond 20 degrees, yaw angle is typically reduced by only about 20%.

While the scope of this paper is not to study the effectiveness of the various drafting formations, a few interesting conclusions are worth noting. First, note that several of the airspeed ratio outliers are due to the echeloned formations, which over-performed (lower airspeed ratio) at high yaw and under-performed at low yaw. For example, the open orange circles (unecheloned) vs the closed orange circles (echeloned) or the open green triangles (unecheloned) vs the closed green triangles (echeloned). Second, note that the simulated peloton (blue diamonds) was not the clear winner. Finally, note the difference in a double paceline where the drafting rider is on the windward (open red squares) and non-windward (closed red squares) side of the group.

Applying these general trends in drafting effects (both airspeed and yaw) to our wind tunnel data, we can re-scale Madone's power savings from a solo wind tunnel condition to the various drafting conditions. As we see in the following figure, drafting generally has less of an effect at higher yaw angles (windier conditions), which is where the Madone really shines aerodynamically.

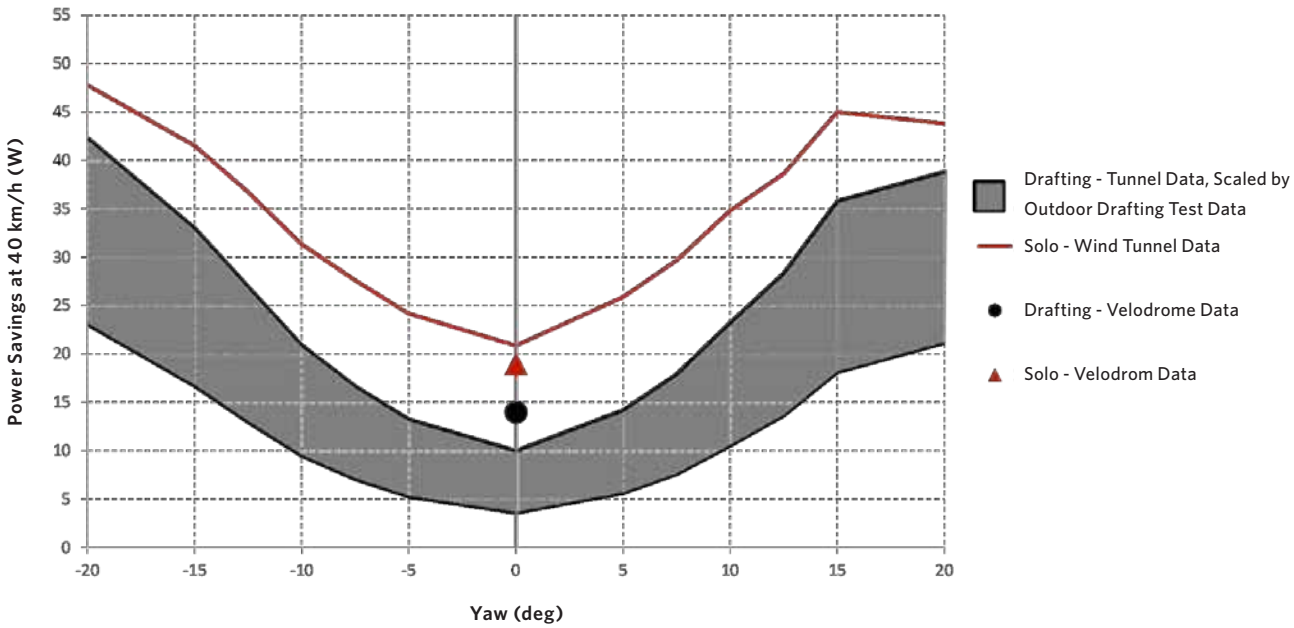

For simplicity, the airspeed in the bike direction is assumed to be the same as the bike speed (thus assuming the ambient wind is a 90 degree side wind).

We also see that the Madone performed better while drafting in the velodrome than in our calculation based on wind tunnel and outdoor drafting test data. One possible explanation is that even on an indoor velodrome, yaw angle can range up to 10 degrees[1], due to the turns. Furthermore, as previously noted we measured the drafting bike's airspeed at just one point at the very front of the bike, likely in the very best portion of the draft zone.

Thus, we believe that our airspeed data is very conservative (does not short-change the effect of drafting). This is supported by the powermeter data, which indicates that the athlete/bike system as a whole generally sees a higher average airspeed than our Aerostick measurement location.

1. Burke, Edmund. *High-tech cycling, 2nd ed.* Human Kinetics (2003).

Effect of drafting distance

During outdoor drafting testing on the 7 km/h wind day, we measured the drafter/leader airspeed ratio of a 2-man formation with a drafting gap ranging from 0 to 4 bike lengths. We found that airspeed is cut in half at a 0 bike length gap and quickly drops off at a 1-2 bike length gap.

The airspeed ratio then asymptotically approaches 100% and is above 95% by 4 bike lengths. 4 bike lengths equates to about 7 meters, but keep in mind that this distance was not precisely measured during the test.

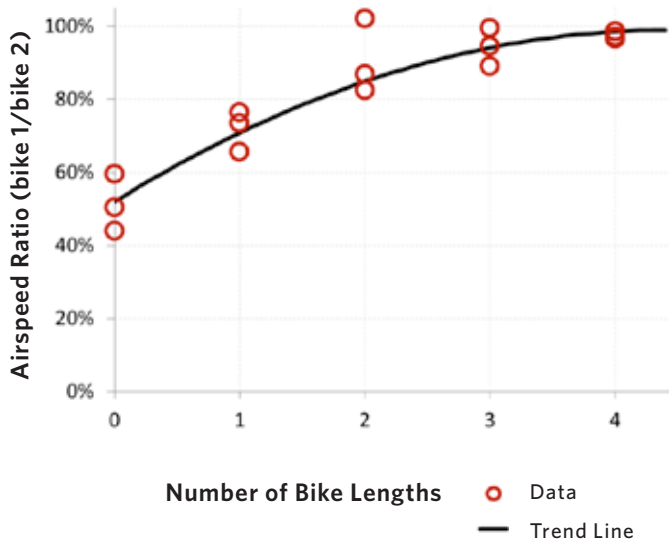

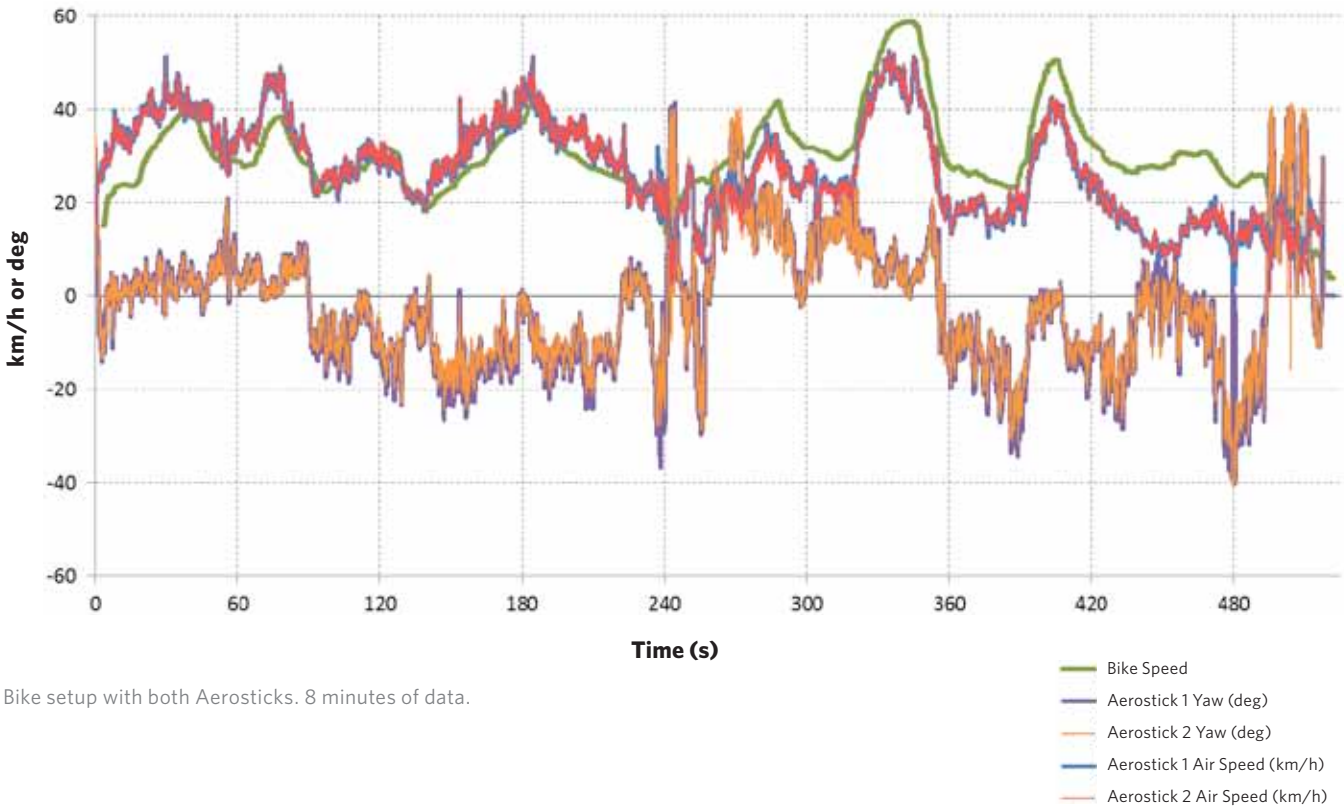

Bike setup with both Aerosticks. 8 minutes of data.

Dual Aerostick validation

As described in section 3.5 of the 2013 Trek Speed Concept White Paper, Trek has gone to extra lengths to create a secondary on-bike calibration for our Aerosticks. As an additional validation that both Aerosticks agree with each other, we mounted both sticks to the same bike and rode in a variety of speed and yaw conditions. As we see above, we were able to achieve very good agreement between the two Aerosticks for both airspeed and yaw measurements.

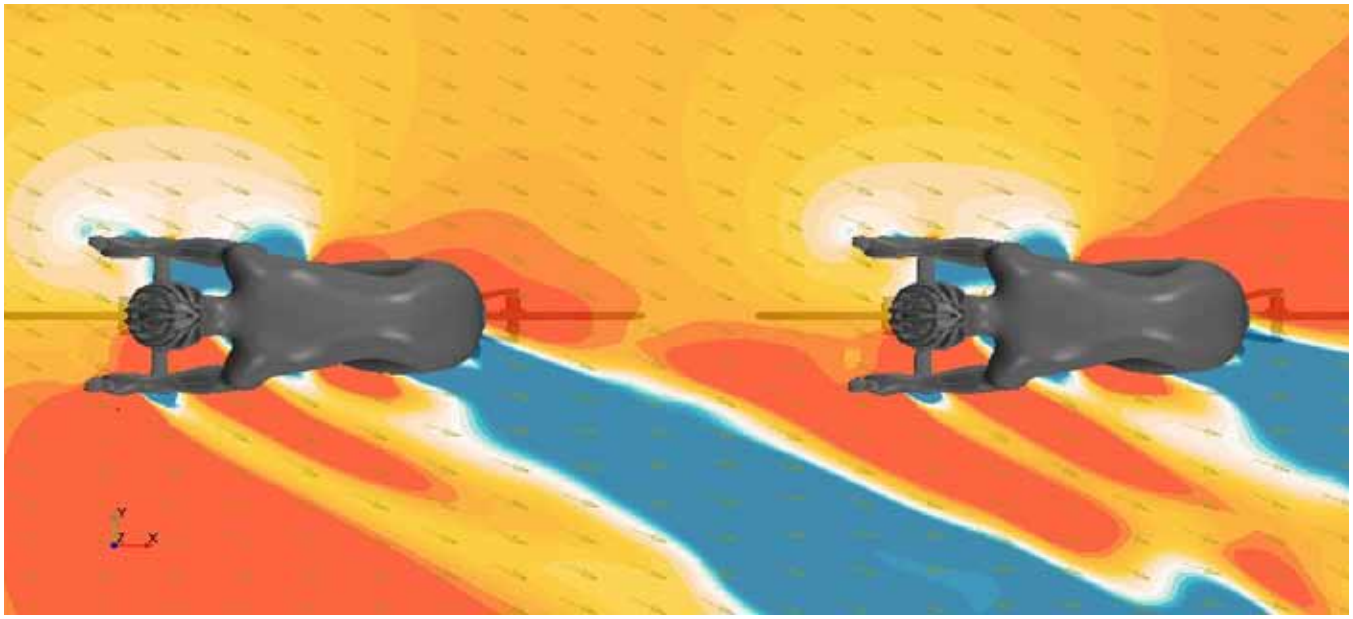

CFD velocities at Aerostick level.

Drafting airspeed ratios greater than 100%

As we've all experienced, echeloning plays a key role in drafting effectiveness at high yaw, so the echeloned vs non-echeloned formations created much of the data spread. As we see above in a transient 3D CFD simulation of a 2-man break at 30 degrees yaw, improper echeloning can put the drafting rider into a region of unaffected airflow (tan) or even accelerated airflow (red). This simulation also verifies the result that yaw, while not immensely impacted by the lead rider, is somewhat reduced in the blue wake region (notice that the arrows become a bit more horizontal in the blue wake zone.)

The following raw data plot shows how the drafting bike's airspeed can equal or even slightly exceed the leading bike's airspeed. This scenario typically exists at high yaw angle in a formation that is not tolerant to high yaw angles.

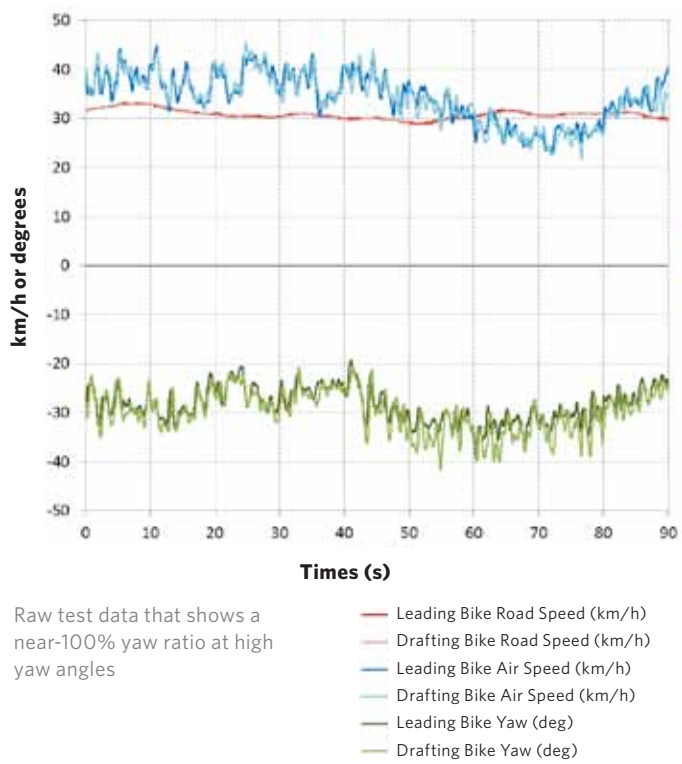

Raw test data that shows a near-100% yaw ratio at high yaw angles

Yaw fluctuation in the raw data

The following raw data plot shows how yaw fluctuation can increase when drafting. When the yaw angle is generally low, this fluctuation can increase the absolute average yaw angle.

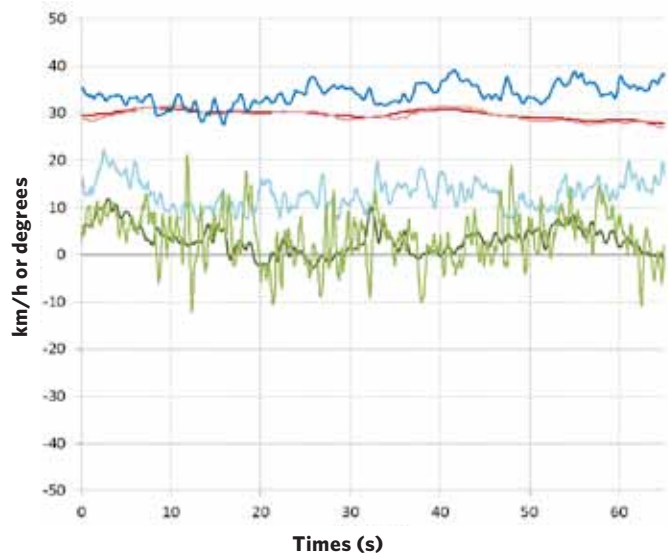

Raw test data that shows increased yaw (and airspeed) fluctuation in the draft.

- Leading Bike Road Speed (km/h)
- Drafting Bike Road Speed (km/h)
- Leading Bike Air Speed (km/h)
- Drafting Bike Air Speed (km/h)
- Leading Bike Yaw (deg)
- Drafting Bike Yaw (deg)

Airspeed ratio trends in the raw data

The following raw data plot shows how the drafting bike airspeed is significantly reduced at low yaw but tends to match the leading bike airspeed when yaw becomes high (in either the positive or negative direction). For example, notice how at 18 seconds, the yaw angle increases for a short period, causing the airspeeds to come together, effectively increasing the airspeed ratio. While this increase in the drafting bike's airspeed may be avoidable by adjusting the echeloning positions, often the yaw angle changes for only 5 or 10 seconds at a time.

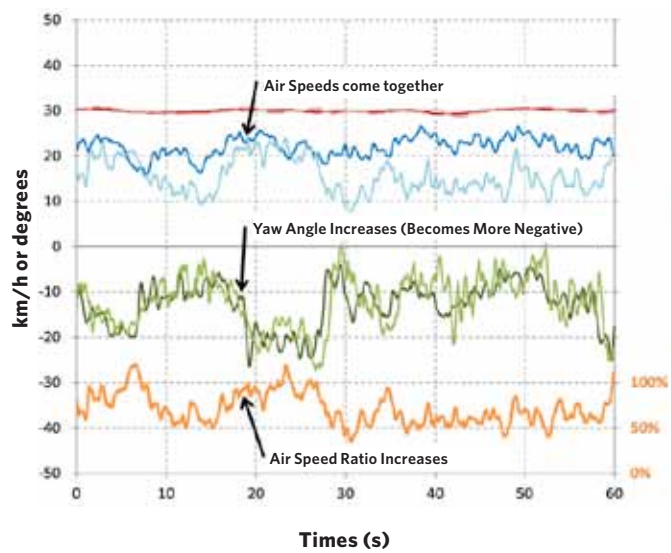

Raw test data that shows the relationship between airspeed ratio and yaw

- Leading Bike Road Speed (km/h)
- Drafting Bike Road Speed (km/h)
- Leading Bike Air Speed (km/h)
- Drafting Bike Air Speed (km/h)
- Leading Bike Yaw (deg)
- Drafting Bike Yaw (deg)
- Airspeed Ratio (Right Axis)

MADONE

TREKBIKES.COM/MADONE

TREK